Gas-Liquid Two-Phase Flow in a Taylor Vortex Flow Reactor

Kenji Ymawaki[1], Hiroyuki Hosoi[2], Teiji Takigawa[3], Mohamed Nabil Noui-Mehidi[4] and Naoto Ohmura[1]

[1]Department of Chemical Science and Engineering, Kobe University,
1-1 Rokkodai, Nada, Kobe 657-8501, Japan
[2]Graduate School of Science and Technology, Kobe University
1-1 Rokkodai, Nada, Kobe 657-8501, Japan
[3] Process Research Laboratories, Kashima Plant, Eisai Co. Ltd.,
22-Sunayama, Hasaki-machi, Kashima, Ibaraki 314-0255, Japan
[4] Energy and Thermofluids Engineering, CSIRO
P.O. Box 56 Highett, Victoria 3190 Australia

The present work experimentally investigates gas-liquid two-phase flow in a Taylor vortex flow reactor. The flow patterns were classified into three flow regimes: bubble dispersion flow (BDF), cellular vortex flow (CVF) and helical vortex flow (HVF). In CVF, the axial wavelength was almost always shorter than in HVF. This indicates that CVF contains more vortex cells than HVF. Consequently, the mean residence time of bubbles is longer in CVF than in HVF. No distinct mixing region could be observed in either CVF or HVF. The tracer diffused axially in an almost one-dimensional diffusion process. It has been found that axial mixing in bubbly flow is considerably different from that in single-phase flow.

1. Introduction

Recent progress in biotechnology makes a dispersed gas-liquid two phase flow more significant in chemical engineering. Higher gas holdup and higher dispersion gas phase is necessary so as to intensify mass transfer between two phases. Moreover, lower shear stress is preferable for bioprocesses to avoid damaging shear-sensitive materials. Due to intense local mixing with limited axial dispersion, Taylor vortex flow (TVF) has potential for a wide range of applications to chemical processes such as emulsion polymerization (Kataoka et al., 1995), crystallization (Jung et al., 2005), culture of tissues (Haut et al., 2003) and photocatalytic reactions (Dutta and Ray, 2004). In many cases of the applications of TVF, as can be seen from the above-mentioned examples, those flows are multiphase systems. Recently much attention has, therefore, been paid to Taylor vortex flow for multiphase systems. A gas-liquid two-phase flow is especially interesting as variety flow states can be observed owing to interaction between centrifugal and buoyancy forces. Shiomi et al. (1993) and Murai et al. (2005) investigated gas-liquid two-phase vertical flow and identified bubbly, spiral and ring flows. Atkhen et al. (2000) also investigated bubbly flow patterns in a vertical Taylor vortex flow system with superimposed axial flow and an upper free surface. Hubacz and Wronskí (2004) also observed bubbly flow patterns in a horizontal Taylor vortex

flow system. Prior to their observation of flow patterns, they studied mass transfer characteristics and revealed that high value of the mass transfer coefficient was obtained (Dluska et al., 2001; Wronskí et al.,2005). Most of the above-mentioned studies were, however, conducted under relatively high rotational Reynolds number conditions, i.e. in turbulent flow regimes. When dealing with shear sensitive materials, mild and effective mixing is favorable. The present work, therefore, experimentally investigates gas-liquid two-phase flow in a Taylor vortex flow reactor without axial liquid flow, under low Reynolds number conditions.

2. Experimental

The experimental apparatus with measuring system is shown in Figure 1. The apparatus consists of an outer cylinder of transparent acrylic resin and an inner cylinder of stainless steel. The outer diameter of the inner cylinder, D_i, is 50 mm($=2R_i$) and the inside diameter of the outer cylinder, D_o, is 76 mm($=2R_o$). The effective length of the annular space is 300 mm. The Reynolds number is defined as $Re=R_i\omega d/v$, where ω is angular velocity [rad/s], d is gap width [m], v is kinematic viscosity [m^2/s]. The critical Reynolds number for the present radius ratio ($\eta = 0.658$) can be estimated to be $Re_c=$ 75.6 by the linear stability theory (Di Prima and Swinney, 1981). An aqueous solution of glycerol is used as the working fluid. The density and viscosity of working fluid were $\rho = 1150$ kg/m^3 and $\mu = 8.14 \times 10^{-3}$ Pa·s, respectively. In order to generate uniform bubbles with diameter of $1 - 1.5$ mm, a compressor drives air through a sparger from the bottom of the apparatus. The volumetric flow rate of gas, V_G, is controlled by a needle valve and set at $5.0 \times 10^{-7} - 3.0 \times 10^{-6}$ m^3/s. The rotational speed of the inner cylinder is varied from $70 - 300$ rpm corresponding to $Re = 336 - 1442$. After the inner cylinder has reached a certain rotational speed, each experiment is performed with an adequate time for vortical structures to form. Four different experiments are conducted: 1) observation of bubbly flow patterns, 2) measurement of the axial wavelength of vortex cells by a flow visualization technique with fine metallic platelet powder (aluminum paint pigment), 3) measurement of liquid height with aeration, and 4) observation of axial mixing behaviors by a flow-visualization technique with fluorescent green dye. In the flow-visualization experiments, the sequential visual data were taken by a digital video camera.
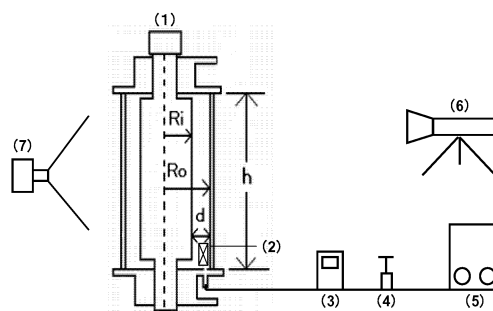
(1) Taylor vortex flow device, (2) sparger,
(3) flowmeter, (4) valve, (5) compressor,
(6) video camera and (7) laser
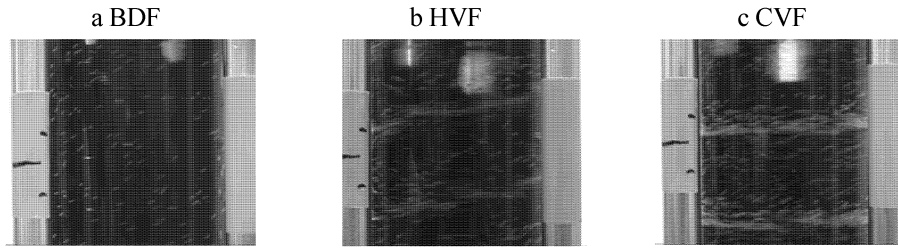
Fig.1 Experimental apparatus

a BDF   b HVF   c CVF

Fig.2 Photographs of flow states

3. Results and Discussion

3.1 Flow patterns

The typical examples of observed flow patterns in the present experiments are shown in Figure 2. At a fixed gas flow rate, the bubbles are dispersed uniformly in the whole region of the test section under low rotational Reynolds number condition, owing to weak centrifugal force compared with buoyancy force (Figure 2 a). This flow pattern is referred to as the bubble dispersion flow (BDF) after the fashion of Shiomi *et al.* (1993). With increase of Reynolds number, there appeared a spiral stripe pattern of bubbles, as shown in Figure 2 b. In this study, this flow pattern is referred to as the helical vortex flow (HVF). Shiomi *et al.* (1993) also observed several spiral flow patterns, i.e. single-spiral flow, double-spiral flow and triple-spiral flow patterns. In the present work, however, only single-spiral pattern was observed. These observations by Shiomi *et al.* (1993) were conducted under higher bubble density and higher rotational Reynolds number conditions than in the present work. The variety of spiral flow pattern observed by Shiomi *et al.* (1993) may be attributed to higher bubble density and turbulent flow structure in Taylor vortex flow. With further increasing of Reynolds number, cellular vortices appeared owing to strong centrifugal force compared with buoyancy force. The bubbles form horizontal rings, as shown in Figure 2 c. This flow pattern is referred to as the cellular vortex flow (CVF). The flow states observed are presented in the diagram of gas flow rate, V_G, against Reynolds number in Figure 3. As can be seen from Figure 3, the Reynolds numbers at which transition from one flow state to another occurs almost linearly increase with gas flow rate. This result indicates that gravitation (the buoyancy) force additionally stabilizes the flow structure in vertical Taylor vortex flow.
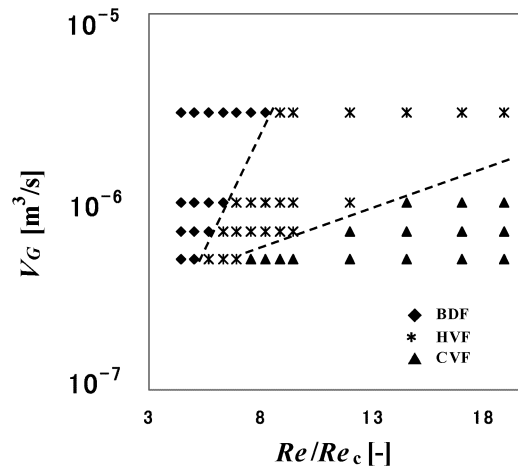

Fig.3 Diagram of flow states

3.2 Axial wavelength

To characterize HVF and CVF, mean axial wavelength was measured by the flow visualization technique with aluminum paint pigment. Figure 4 shows the dimensionless mean axial wavelength, λ/d, plotted against the rotational Reynolds number divided by the critical Reynolds number, Re/Re_c, with gas flow rate. As shown in Figure 4, λ/d almost linearly decreases with increasing Re/Re_c under the same flow state. Decreasing ratio of λ/d is steeper in CVF than in HVF. Furthermore, the axial wavelength in CVF is almost always smaller than in HVF.

3.3 Mean residence time of gas

The present work obtained the mean residence time of gas, τ, by measuring liquid height with aeration. τ is determined by the following equation:

$$\tau = \frac{\pi\left(R_o^2 - R_i^2\right)\Delta H}{V_G} \tag{1}$$

where ΔH [m] is the difference of liquid height between with and without aeration. Figure 5 shows dependence of Re/Re_c on τ. As expected, τ increases with Re/Re_c. This result suggests that a larger amount of bubbles can be captured by a larger centrifugal force. From the flow-visualization experiments, many bubbles were captured in the outflow regions along the inner cylinder, as Shiomi et al. (1993) reported. On the other hand, some bubbles were trapped within the vortex core. This phenomenon was firstly reported Deng et al. (2006). As mentioned in the previous section, the axial wavelength in CVF is almost always smaller than in HVF and the decreasing ratio of λ/d is steeper in CVF than in HVF. This indicates that CVF contains more vortex cells in the axial direction than HVF and that the number of vortex cells increases more rapidly with Re/Re_c in CVF than in HVF. These features can be expressed in Figure 5, i.e. τ is always longer and the increasing ratio of τ is steeper than in HVF.
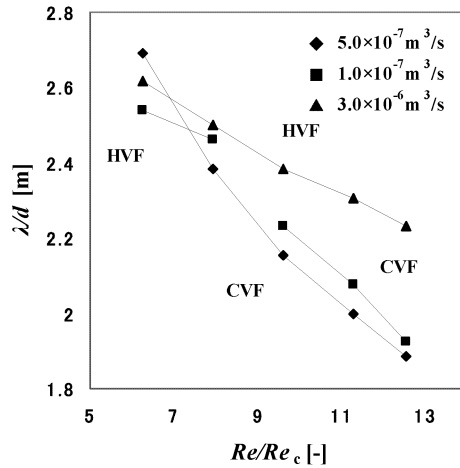
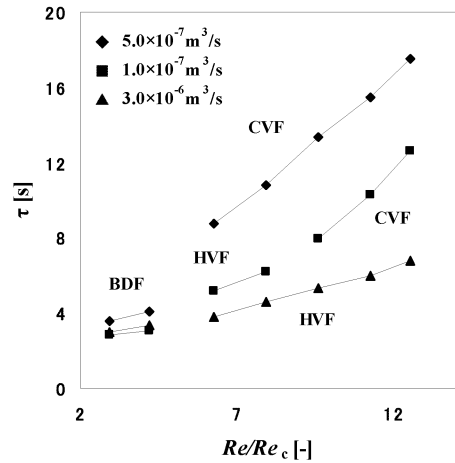

Fig.4 λ/d against Re/Re_c

Fig.5 τ against Re/Re_c

3.4 Axial mixing behaviors

The effect of bubbles on axial mixing behaviors was examined by flow-visualization experiments with fluorescent green dye. Figure 6 shows cross-sectional views presenting axial diffusion process of tracer. The flow-visualization experiment by a laser-induced fluorescence method clearly revealed that there exist two distinct mixing regions at low Reynolds numbers in the single-phase Taylor vortex flow, as shown in Figure 6 a. The tracer near the vortex cell boundary was rapidly transported downward in the axial direction owing to the bypass flow effect, while the fluid element was confined to the vortex core region without being exchanged with the outer flow region. On the other hand, in the case of bubbly flow, no distinct mixing region could be observed in either CVF or HVF. The tracer diffused axially in an almost one-dimensional diffusion process. These results indicate that the axial mixing in bubbly flow is considerably different from that in single-phase flow.
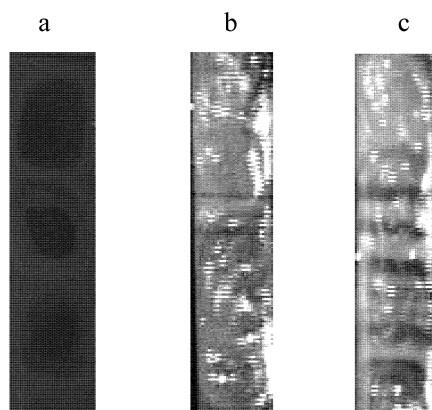

Fig.6 Cross-sectional views of axial diffusion of tracer green dye : a single-phase flow, b HVF and c CVF

4. Conclusion

The present work experimentally investigates gas-liquid two-phase flow in a Taylor vortex flow reactor. The flow patterns were classified into three flow regimes: bubble dispersion flow (BDF), cellular vortex flow (CVF) and helical vortex flow (HVF). When Re was small, the centrifugal force was so weak that bubbles were uniformly dispersed in the annulus at all gas flow rates. As Re increased, the centrifugal force and the buoyancy force became comparable and HVF was obtained. Bubbles were distributed near the inner cylinder and formed a helical-band structure. With further increase of Re, the centrifugal force due to the inner cylinder was stronger than the buoyancy force and CVF was observed. In CVF, the axial wavelength was almost always shorter than in HVF. This indicates that CVF contains more vortex cells than HVF. Consequently, the mean residence time of bubbles is longer in CVF than in HVF. No distinct mixing region could be observed in either CVF or HVF. The tracer diffused axially in an almost one-dimensional diffusion process. The axial mixing in bubbly flow is considerably different from that in single-phase flow. Many attempts at applying Taylor vortex flow in chemical processes were based on the assumption of plug-flow like mixing characteristics, i.e. low value of the axial dispersion with respect to the radial dispersion. In gas-liquid two-phase vertical Taylor vortex flow, however, this assumption may not be applicable.

5. References

Atkhen, K., Fontaine, J. and Wesfreid, J. E., 2000, J. Fluid Mech., 422, 55.

Deng, R., Wang, C-H. and Smith, K. A., 2006, Phys. Rev. E, 73, 036306

Dluska, E., Wronski, S. and Hubacz, R., Chem. Eng. Sci., 2001, 1131.

Dutta, P. K. and Ray, A. K., 2004, Chem. Eng. Sci., 59, 5249.

Haut, B., Amor, H. B., Coulon, L., Jacquet, A. and Halloin, V., Chem. Eng, Sci., 2003, 58, 777.

Hubacz, R. and Wronski, S., 2004, Experimental Thermal & Fluid Science, 2004, 28, 457.

Jung, T., Kim, W-S. and Choi, C. K., 2005, Cryst. Res. Technol., 40, 586.

Kataoka, K. Ohmura, N., Kouzu, M., Simamura, Y. and Okubo, M., 1995, Chem. Eng. Sci., 50, 1490.

Murai, Y., Oiwa, H. and Takeda, Y., 2005, J. Phys. :Conference Series, 14, 143

Shiomi, Y., Kutsuna, H., Akagawa, K. Ozawa, M., 1993, Nucl. Eng. Des., 141, 27.

Wronski, S., Hubacz, R., Ryszczul, T., 2005, Chem. Eng. J., 105, 71.